USING GABOR DICTIONARIES IN A $TV - L^\infty$ MODEL, FOR DENOISING

Tieyong Zeng, François Malgouyres

LAGA/L2TI, Université Paris 13
99 avenue Jean-Batiste Clément, 93430 Villetaneuse, France
E-mail: {zeng,malgouy}@math.univ-paris13.fr

ABSTRACT

The goal of this paper is to report on experiments where we use Gabor dictionaries in a $TV - l^\infty$ model for denoising. This allows many possible choices. Our conclusions are that the choice of the dictionary mostly impact the restoration of textures. Moreover, for most images, better results are obtained when the Gaussian term of the Gabor filters is close to isotropic.

1. INTRODUCTION

By image denoising we mean the recovery of a datum $u \in \mathbb{R}^{N^2}$ from a measurement $v = u + b$, where $b \in \mathbb{R}^{N^2}$ is a Gaussian white noise of standard deviation σ.

For few years, some authors have been investigating the solution provided by the following model :

$$\begin{cases} \text{minimize } TV(w) \\ \text{under the constraint } \|w - v\|_{\mathcal{D},\infty} \leq \tau \end{cases} \tag{1}$$

where $\|.\|_{\mathcal{D},\infty}$ is defined by

$$\|u\|_{\mathcal{D},\infty} = \sup_{\psi \in \mathcal{D}} |\langle u, \psi \rangle|,$$

for a finite dictionary $\mathcal{D} \subset \mathbb{R}^{N^2}$ and a discretization of the total variation (see references below for details).

This model has, at least, been studied in [1, 2, 3, 4]. (Those references are listed in the chronological order of disclosure, the content of these papers is summarized in the introduction of [4].) Notice that (1) can be used for image restoration (when u also undergo a linear distortion). Though, for simplicity and clarity, we do not consider this situation in this paper.

The purpose of the current paper is to understand how to chose the dictionary, in order to improve the results of (1). In this regard, the authors of [2] tried a curvelet dictionary and conjectured it is the best possible choice. The authors of [1, 3, 4] tried a wavelet packet dictionary.

In order to make experiments for several kinds of dictionary, we tried dictionaries made of Gabor functions. The motivations for this choice are of two natures. First, as is described in the next section, they allow many possibilities for frequencial and spacial localization. Secondly, they are often used to describe texture and we believe that $\mathcal{D}$ should have this property.

The reason for this belief is that the Kuhn-Tucker equation satisfied by the solution u^* to (1) is

$$\nabla TV(u^*) = \sum_{\Psi \in \mathcal{D}} \lambda_\Psi \Psi$$

for some real numbers $(\lambda_\Psi)_{\Psi \in \mathcal{D}}$. Moreover, if an element Ψ is such that $\lambda_\Psi \neq 0$, we know that $\langle w - v, \Psi \rangle = \tau$. This means that, in order to solve (1), we had to erase, as much as possible, the information modelled by Ψ (which is bad). So, for a good dictionary there should exists a sparse representation of $\nabla TV(u^*)$ in $\mathcal{D}$. When interpreted in the context of $BV([0, N]^2)$ (the space of bounded variation, see, for instance [5]), this means that the dictionary should give a good description of the dual of BV. The latter is often considered for texture modeling (see [5] and [6] and references therein).

Notice the above heuristic is confirmed by the experimental results described in Section 5 : While we tested 12 different dictionaries, they all provide similar results on homogeneous zones and in the vicinity of edges. The only differences occur in textured zones.

Moreover, we found that, for Gabor dictionaries, the shape of the elements of the dictionary (σ and σ', in (3)) should not relate to their frequency location (f, in (3)). This is, at least, true for images in which the texture patterns are not related to the shape of the region where the texture lives.

2. THE DICTIONARY

2.1. From features to dictionary

In order to build the dictionary, we first consider a finite set

$$\mathcal{F} = \{\psi^k\}_{1 \leq k \leq r}$$

of elements of $\mathbb{R}^{N^2}$. In the remaining of the paper, we refer to these elements as "features".

For any $k \in \{1, \ldots, r\}$ and any indexes $(i, j) \in \{0, \ldots, N-1\}^2$, we denote

$$\Psi^{k,i,j}_{m,n} \triangleq \Psi^k_{m-i,n-j}, \tag{2}$$

where $(m,n) \in \{0,\dots,N-1\}^2$, the translation of Ψ^k. (Notice the images and features are periodized out of $\{0,\dots,N-1\}^2$.)

We then consider the dictionary

$$\mathcal{D} = \{\Psi^{k,i,j}, \text{for } 1 \le k \le r \text{ and } 0 \le i,j < N\}.$$

The dictionary $\mathcal{D}$ is obviously translation invariant. Moreover, depending on the features it can also be rotation invariant, scale invariant,...

3. THE FEATURES

Again, the considered features are Gabor filters, they are of the form

$$g^{f,\theta}_{m,n} = Ce^{-\frac{x^2}{\sigma}-\frac{y^2}{\sigma'}}\cos(2\pi\frac{f\,x}{N}), \tag{3}$$

where f and $\theta \in \mathbb{R}$, σ and σ' need to be chosen, $x = m\cos\theta + n\sin\theta$, $y = -m\sin\theta + n\cos\theta$ and C is such that the l^2 norm of the features equal 1.

Knowing the features take the form (3), we still need to determine the frequency and angular locations of these elements.

Except for the features described in section 3.4, we consider a finite set of frequencies $\{f_{f_l}\}_{0\le f_l\le F}$. We then split the frequency band characterized by f_{f_l} (or f_l) in A_{f_l} angular sections. For this band, we obtain A_{f_l} features

$$g^{f_{f_l},\theta_a} \tag{4}$$

where $\theta_a = \frac{2\pi a}{A_{f_l}}$, for $a \in \{0,\dots,A_{f_l}-1\}$.

Once these locations are fixed, σ and σ' are chosen so that the Fourier transforms of the features cover the whole disk of center 0 and radius $\frac{N}{2}$. (Of course, we would gain in covering the whole Fourier domain.) Moreover, σ and σ' are fixed automatically so that the Fourier transforms of any two features do not too much overlap. Notice that, given (4), there is no need to adapt the variances σ and σ' to the angular direction. We therefore have a bench of $(\sigma_{f_l},\sigma'_{f_l})_{0\le f_l\le F}$.

The sum of the Fourier transforms of the features described below are represented on Figure 1.

3.1. Features of type Gabor I

We call Gabor I features those build according to (4) where, for non-negative integers F and A, we take, for $f_l \in \{0,\dots,F\}$,

$$\begin{cases} f_{f_l} = 0 \text{ and } A_{f_l} = 1 & \text{, if } f_l = 0, \\ f_{f_l} = \frac{3}{8}2^{f_l-F} \text{ and } A_{f_l} = A & \text{, otherwise.} \end{cases}$$

We then take, for $f_l \in \{0,\dots,F\}$,

$$(\sigma_{f_l},\sigma'_{f_l}) = \begin{cases} \left(C(\frac{2^F}{N})^2, C(\frac{2^F}{N})^2\right) & \text{, if } f_l = 0 \\ \left((C(\frac{42^F}{N2^{f_l}})^2, C(\frac{A_{f_l}}{2\pi f_{f_l}})^2\right) & \text{, otherwise,} \end{cases} \tag{5}$$

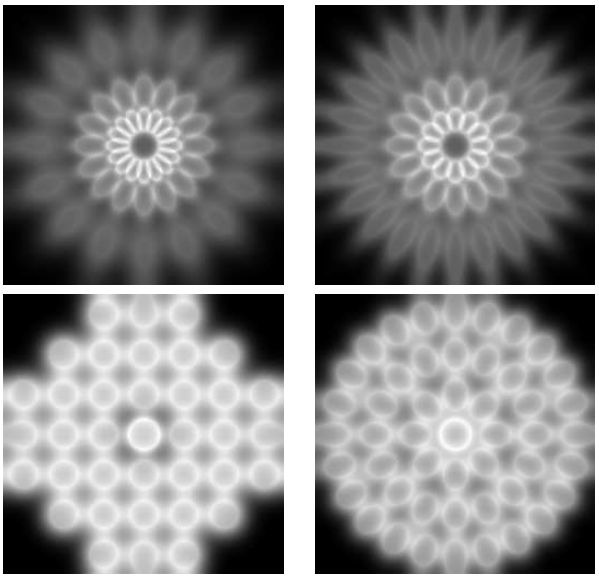

Fig. 1. Sum of the Fourier transforms of the : Up-left : Gabor 1 features; Up-Right : features with curvelet scaling; Bottom-Left : Gabor 3 features; Bottom-Right : Gabor 2 features.

with $C = \frac{4N^2 log(a^{-1})}{\pi^2}$, with a is a constant, in our experiments, we let $a = 0.15$. (The value of C is such that, once normalized, the Fourier transform of $e^{-\frac{x^2}{C(x')^{-2}}} = a$ at the frequency x'.)

3.2. Features of type Gabor II

For non-negative integers F and A, we take, for $f_l \in \{0,\dots,F\}$,

$$\begin{cases} f_{f_l} = 0 \text{ and } A_{f_l} = 1 & \text{, if } f_l = 0, \\ f_{f_l} = f_l\frac{N}{2F+1} \text{ and } A_{f_l} = f_l A & \text{, otherwise.} \end{cases}$$

The variances $(\sigma_{f_l},\sigma'_{f_l})$ equal

$$(\sigma_{f_l},\sigma'_{f_l}) = \begin{cases} (C(\frac{2F+1}{N})^2, C(\frac{2F+1}{N})^2) & \text{, if } f_l = 0 \\ (C(\frac{2F+1}{N})^2, C(\frac{A(1F+1)}{2\pi N})^2) & \text{, otherwise,} \end{cases}$$

where C is as in (5).

3.3. Features with a curvelet scaling

For details on the curvelet scaling, see [2] and references therein. For non-negative integers F and A, we take, for $f_l \in \{0,\dots,F\}$,

$$\begin{cases} f_{f_l} = 0 \text{ and } A_{f_l} = 1 & \text{, if } f_l = 0, \\ f_{f_l} = \frac{3N}{8}2^{f_l-F} \text{ and } A_{f_l} = rd\left(A2^{\frac{f_l-F}{2}}\right) & \text{, otherwise,} \end{cases}$$

where $rd(t)$ is the closest integer to t.

The variances $(\sigma_{f_l},\sigma'_{f_l})$ are determined according to (5).

3.4. Features of Gabor type III

This cosine dictionary, is similar to fully decomposed wavelet packet basis of a given depth. It has the advantage of being translation invariant.

For $F \in \mathbb{N}$, we consider the set of frequency locations

$$\mathcal{F}' = \left\{ \left(i\frac{N}{2F}, j\frac{N}{2F} \right), \text{ with } i \in \{0, \dots, F\}, \right.$$
$$\left. j \in \{-F, \dots, F\} \text{ and } i^2 + j^2 \leq \frac{N^2}{4} \right\}$$

The set of features is then of the form

$$\mathcal{F} = \left\{ e^{-\frac{n^2+m^2}{\sigma}} \cos(2\pi(f_x m + f_y n)), \text{ for } (f_x, f_y) \in \mathcal{F}' \right\},$$

for $\sigma = C(\frac{2F+1}{N})^2$, where C is as in (5). (Notice the elements corresponding to $i = 0$ appear twice, in $\mathcal{F}$. This should be fixed before (1) is actually solved.)

4. NUMERICAL ASPECTS

We use a penalty method, in order to solve (1). More precisely, we minimize the unconstrained energy

$$TV(w) + \lambda \sum_{\Psi \in \mathcal{D}} \varphi_\tau(\langle w - v, \Psi \rangle), \tag{6}$$

with

$$\varphi_\tau(t) = (\sup(|t| - \tau, 0))^2,$$

and for a large number λ.

This optimization problem is solved by a steepest descent algorithm. In order to get such an algorithm, the main difficulty id to compute the gradient of (6). It takes the form

$$\nabla TV(w) + \lambda \sum_{\Psi \in \mathcal{D}} \varphi'_\tau(\langle w - v, \Psi \rangle)\Psi,$$

where φ'_τ denotes the derivative of φ_τ.

We do not detail how to compute $\nabla TV(w)$. It can easily be found in the literature. In order to compute the gradient of the data fidelity term we need to compute the decomposition in $\mathcal{D}$ and a recomposition. These two operations are detailed in the next two sections.

4.1. The decomposition

The decomposition of $u \in \mathbb{R}^{N^2}$ provides the set of values

$$(\langle u, \Psi_{k,i,j} \rangle)_{0 \leq i,j < N} \text{ and } {}_{1 \leq k \leq \#\mathcal{F}}.$$

Notice that, using (2), we have, for any $u \in \mathbb{R}^{N^2}$ and any feature $\Psi^{k,i,j} \in \mathcal{F}$,

$$\langle u, \Psi^{k,i,j} \rangle = \sum_{m,n=0}^{N-1} u_{m,n} \Psi^k_{m-i,n-j}.$$

type/size	small	medium	large
Gabor I, $(F, A) =$	(3,8)	(3,16)	(3,48)
Gabor II, $(F, A) =$	(3,4)	(5,4)	(8,4)
curvelet, $(F, A) =$	(3,6)	(3,10)	(3,32)
Gabor III, $F =$	7	11	18

Table 1. Parameters for the dictionary definitions. The features of small dictionaries are displayed on 1.

So the set of values $(\langle u, \Psi_{k,i,j} \rangle)_{1 \leq i,j < N}$, is just $u * \overline{\Psi^k}$, where $*$ stands for the convolution product and $\overline{\Psi^k}_{m,n} = \Psi^k_{-m,-n}$ (remember the images are periodized).

The decomposition can therefore be computed with one Fourier transform and $\#\mathcal{F}$ inverse Fourier transform, if we memorize the Fourier transforms of the features.

4.2. The recomposition

Denoting $\Lambda = (\lambda^k_{i,j})_{0 \leq i,j < N}$ and ${}_{1 \leq k \leq \#\mathcal{F}}$ and $m = \#\mathcal{F}N^2$, the recomposition takes the following form

$$T : \Lambda \in \mathbb{R}^m \to \sum_{k=1}^{\#\mathcal{F}} \sum_{i,j=0}^{N-1} \lambda^k_{i,j} \Psi^{k,i,j} \in \mathbb{R}^n.$$

Using (2), we get

$$T(\Lambda) = \sum_{k=1}^{\#\mathcal{F}} \lambda^k * \Psi^k$$

This can be computed with $\#\mathcal{F}$ Fourier transforms and one inverse Fourier transform.

5. EXPERIMENTS

We report on denoising experiments of the image "Barbara". The noise variance is $\sigma = 20$. The twelve dictionaries described in Table 1 have been tested. For each dictionary, we tuned the parameter τ (in (1)) in order to obtain good visual results. The images can be found on

$$http://www.math.univ-paris13.fr/\sim zeng/gabor/$$

In this paper we focus on three regions of the images. They corresponds to the white zones on Figure 2. The zones are represented on Figure 3.

Zone 1 contains an edge. All the dictionaries give about the same kind of results (see Table 2).

Zone 2 contains a texture whose orientation is not related to the shape of region where it lives. Gabor II features, whose spacial localization is almost isotropic, give the best results. Features with a curvelet scaling, whose spacial localization

Fig. 2. Barbara image. The most interesting zones are in white.

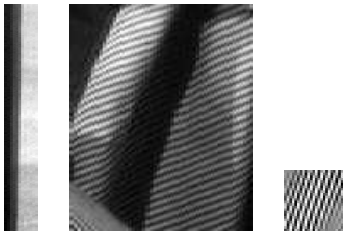

Fig. 3. Left : zone 1; Center : zone 2; Right : zone 3.

type/size	small	medium	large
Gabor I	27.2375	27.1484	27.1073
Gabor II	27.2617	27.1569	26.8859
curvelet	27.2239	27.1711	27. 0189
Gabor III	27.2449	27.1612	26.8798

Table 2. PSNR for zone 1.

Fig. 4. Left : Noisy zone 2; center : result for the medium "curvelet scaling" dictionary, $PSNR = 21.7$; Left : result for the medium Gabor II dictionary, $PSNR = 23.4$.

type/size	small	medium	large
Gabor I	19.4346 9	19.113	21.0173
Gabor II	20.6871	20.0332	21.8354
curvelet	18.7523	21.0859	21.0625
Gabor III	20.4984	17.0148	20.4302

Table 3. PSNR for zone 3.

is strongly anisotropic and fits the texture patterns, give the worst.

Zone 3 contains a texture supported on an elongated region. Moreover, the pattern of the texture fits the shape of the region where it lives. Features with a curvelet scaling or gabor II give better results than the other features. Our belief is that this region might be rare in natural images. Moreover, we can barely see the difference between the images.

Acknowledgment

Part of this work has been performed while Tieyong Zeng was supported by Alcatel espace.

6. REFERENCES

[1] F.Malgouyres, "Minimizing the total variation under a model convex constraint for image restoration," *IEEE, trans. On Image Processing,*, vol. 11(12)), pp. 1450–1456, Dec.2002.

[2] E.Candes and F.Guo, "New multiscale transforms, minimun total variation synthesis: application to edge regularization in image compression," *Signal Processing*, pp. 82(11):1519–1543, 2002.

[3] F. Malgouyres, "Mathematical analysis of a model which combines total variation and wavelet for image restoration," *Journal of information processes*, vol. 2, no. 1, pp. 1–10, 2002, available at http://www.math.univ-paris13.fr/∼malgouy.

[4] S.Lintner and F.Malgouyres, "Solving a variational image restoration model which involves l^∞ contraints.," *Inverse Problem*, vol. 20(3), pp. 815–831, June 2004.

[5] Y. Meyer, *Oscillating paterns in image processing and in some nonlinear evolution equation*, AMS, Boston, MA, USA, 2001, The Fifteenth Dean Jacqueline B. Lewis Memorial Lectures.

[6] J.F. Aujol, G. Gilboa, and S Osher, "Structure-texture image decomposition - modeling, algorithms and parameter section," CAM report 05-10, UCLA, 2005.